

Simplified statistical image reconstruction algorithm for polyenergetic X-ray CT

Somesh Srivastava, *Student member, IEEE*, and Jeffrey A. Fessler, *Senior member, IEEE*

Abstract—In X-ray computed tomography (CT), bony structures cause beam-hardening artifacts that appear on the reconstructed image as streaks and shadows. Currently, there are two classes of methods for correcting for bone-related beam hardening. The standard approach used with filtered backprojection (FBP) reconstruction is the Joseph and Spital (JS) method [1]. In the current simulation study (which is inspired by a clinical head scan), the JS method requires a simple table or polynomial model for correcting water-related beam hardening, and two additional tuning parameters to compensate for bone. Like all FBP methods, it is sensitive to data noise. Statistical methods have also been proposed recently for image reconstruction from noisy polyenergetic X-ray data, [2], [3]. However, these methods have required more knowledge of the X-ray spectrum than is needed in the JS method, hampering their use in practice. This paper proposes a simplified statistical image reconstruction approach for polyenergetic X-ray CT that uses the same calibration data and tuning parameters used in the JS method, thereby facilitating its practical use. Simulation results indicate that the proposed method provides improved image quality (reduced beam hardening artifacts and noise) compared to the JS method, at the price of increased computation. The results also indicate that the image quality of the proposed method is comparable to a method requiring more beam-hardening information [3].

Index Terms—X-ray computed tomography, beam-hardening, Joseph-Spital method, statistical reconstruction techniques.

I. INTRODUCTION

BEAM hardening causes artifacts in X-ray CT images. These artifacts manifest themselves as “cupping” due to water-related beam-hardening and as “streaks” or “shadows” due to bone-related beam-hardening. Current X-ray CT systems are well-calibrated to compensate for water-related beam-hardening. Additional calibration for bone-related beam-hardening is not required as use of a few tuning parameters in addition to the above calibration during the reconstruction phase (using the JS method) is sufficient to compensate for bone-related beam-hardening. As we shall see in a later section, the number of additional parameters required depends on the image viewing range and amount of soft-tissue and bone in the subject being scanned. Earlier statistical methods of [2], [3] require more information about the X-ray spectrum and/or materials being imaged than is available to the standard JS method. Consequently, these algorithms are less easily incorporated into the current X-ray CT systems. This paper proposes a statistical

reconstruction algorithm that uses the same beam-hardening information as the JS method.

II. MODEL

Polyenergetic X-ray CT measurements for the i th ray through the object are assumed to be generated according to the following statistical model :

$$y_i \sim \text{Poisson} \left\{ \int I_i(\mathcal{E}) e^{-\int_{L_i} \mu(x,y,\mathcal{E}) d\ell} d\mathcal{E} + r_i \right\},$$

where, $I_i(\mathcal{E})$ is the energy spectrum of the incident X-rays, $\mu(x, y, \mathcal{E})$ is the X-ray attenuation coefficient for energy \mathcal{E} at location (x, y) in the object, L_i denotes the i th ray through the object and r_i denotes scatter. We assume a two-material model (soft-tissue and bone¹) and express the X-ray attenuation coefficient as the product of mass attenuation coefficient, $m(\mathcal{E})$ and material density, $\rho(x, y)$. Thus, we have,

$$y_i \sim \text{Poisson} \left\{ b_i e^{-f_i(T_S, T_B, i)} + r_i \right\}, \quad (1)$$

$$f_i(T_S, T_B, i) \triangleq -\log \int \frac{I_i(\mathcal{E})}{b_i} e^{(-m_S(\mathcal{E})T_S, i - m_B(\mathcal{E})T_B, i)} d\mathcal{E},$$

$$T_{S, i} \triangleq \int_{L_i} \rho_S(x, y) d\ell \triangleq [GI_S \rho]_i,$$

$$T_{B, i} \triangleq \int_{L_i} \rho_B(x, y) d\ell \triangleq [GI_B \rho]_i,$$

where, $b_i \triangleq \int I_i(\mathcal{E}) d\mathcal{E}$, ρ is a vector consisting of densities for each pixel, I_S and I_B are diagonal matrices representing the image-domain masks for soft-tissue and bone respectively and G is the forward projection operator. Note that $f_i(T_S, T_B)$ is equal to the logarithm of the incident intensity of the X-ray spectrum to the exit intensity. In principle, this table could be measured using step phantoms. We call $f(T_S, T_B)^2$ the water and bone correction table, and $f(T_S, 0) \triangleq f_S(T_S)$ the water correction table.

The method of [3] uses the entire water and bone correction table. This method will be called the Exact method from now on. The JS method utilizes the water correction table and a few tuning parameters. The purpose of the additional parameters is to suitably extrapolate the water correction table to approximate the water and bone correction table within the tolerable error

Supported in part by GE Healthcare Technologies and NIH grant CA87634.

Somesh Srivastava and Jeffrey A. Fessler are with the Electrical Engineering: Systems Dept., University of Michigan, Ann Arbor, MI 48109, USA. (E-mail: someshs@umich.edu, fessler@umich.edu).

¹The terms soft-tissue and water are used interchangeably because the two materials have similar X-ray attenuation properties.

²The subscript i is dropped as each ray has the same incident energy spectrum.

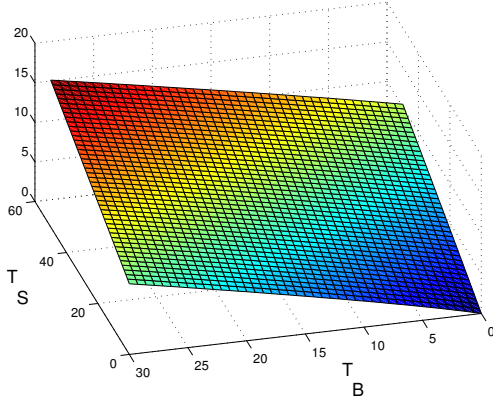


Fig. 1. Plot of $f(T_S, T_B)$. Units of T_S and T_B are g/cm^2 .

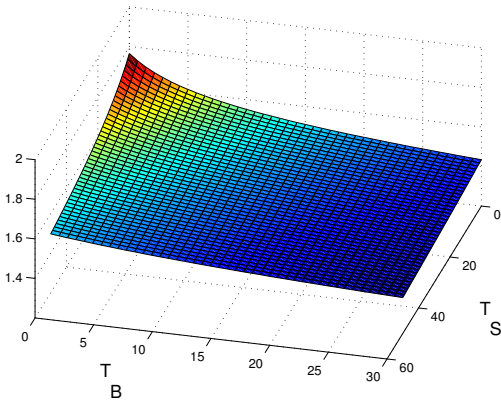


Fig. 2. Plot of $\gamma(T_S, T_B)$. Units of T_S and T_B are g/cm^2 .

range. The proposed method uses the same approximation as the JS method.

This paper is organized as follows. Section III describes the conditions under which $f(T_S, T_B)$ can be approximated using two tuning parameters. Section IV describes the proposed method (the 2-parameter method) and other choices of statistical methods that can be used to eliminate noise and beam-hardening artifacts. The simulation setup is described in Section V and the results and a discussion of the results is presented in Section VI.

III. APPROXIMATING THE WATER AND BONE CORRECTION TABLE

The water and bone correction table, $f(T_S, T_B)$, can be computed exactly in simulations and is shown in Fig. 1. Note that the non-linearity of $f(T_S, T_B)$ is the source of the beam-hardening artifacts. In the current study, $f(T_S, T_B)$ is computed for a 80kVp spectrum and two materials, soft-tissue and bone.

We use the one-to-one nature of the water correction table

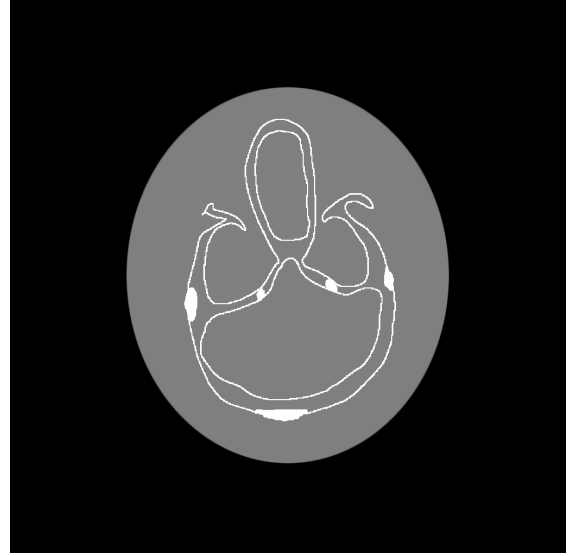


Fig. 3. Image of the true phantom (1024×1024 pixels). Window = 400HU.

f_S in order to rewrite $f(T_S, T_B)$ as :

$$\begin{aligned} f(T_S, T_B) &= f(T_S + \gamma(T_S, T_B)T_B, 0) \\ &= f_S(T_S + \gamma(T_S, T_B)T_B), \end{aligned}$$

where,

$$\gamma(T_S, T_B) \triangleq \begin{cases} \frac{f_S^{-1}(f(T_S, T_B)) - T_S}{T_B} & T_B \neq 0, \\ \lim_{T \rightarrow 0} \frac{f_S^{-1}(f(T_S, T)) - T_S}{T} & T_B = 0. \end{cases}$$

This formulation takes full advantage of the water correction table f_S . Fig. 2 shows the plot of $\gamma(T_S, T_B)$ corresponding to the $f(T_S, T_B)$ shown in Fig. 1. The function $\gamma(T_S, T_B)$ is equivalent to λ_L defined in Eq.(13) of [1]. An accurate approximation of $\gamma(T_S, T_B)$ by a function of two variables (T_S and T_B) involving the tuning parameters is required for a good reconstruction.

The number of tuning parameters needed for the approximation to $\gamma(T_S, T_B)$ depends on the amount of tolerable error. The error tolerance depends on the image viewing window. We focus here on a 400 HU window (or 0.4g/cc in density units). The phantom also plays a role in the choice of number of tuning parameters. This is because the approximation to $\gamma(T_S, T_B)$ has to be good over the range of T_S and T_B determined by the amounts of soft-tissue and bone in the phantom. The phantom in this simulation study is designed based on a clinical case.

In the current study, we use the following approximation for $\gamma(T_S, T_B)$:

$$\gamma(T_S, T_B) \approx A - BT_B, \quad (2)$$

which is identical to Eq.(22) of [1]. The plot of $\gamma(T_S, T_B)$ in Fig. 2 suggests that the above approximation could be reasonable. It will be shown through simulations that this approximation works well for the head phantom. The thickness of bone mineral in the head phantom is around 1.5mm.

Increasing the bone mineral thickness to about 2.5mm causes this approximation to fail, necessitating the use of more tuning parameters. We consider only the 1.5mm case in this paper.

IV. STATISTICAL RECONSTRUCTION METHODS

We compare the following statistical reconstruction methods.

1) 1-parameter method

We use a constant to approximate $\gamma(T_S, T_B)$ instead of using (2), *i.e.*, set $B = 0$. This is equivalent to Eq.(20) of [1]. This method is used to verify that the amount of bone in the phantom is significant from the point of view of beam-hardening, and more than one tuning parameter is required for the approximation to be good.

2) 2-parameter method

This is the proposed method and uses (2) to approximate $\gamma(T_S, T_B)$.

3) Exact method

The exact value of $\gamma(T_S, T_B)$, hence the exact value of $f(T_S, T_B)$, is known in simulations. This method is almost identical to [3].

4) Ad hoc method

In this method, we perform the statistical reconstruction assuming a water-correction model and process the obtained image by the JS method. We assume that the noise can be removed by including the water correction model (*i.e.* set $A = 1$ and $B = 0$) only in the measurement model. Now, the JS method is used to get rid of the beam-hardening artifacts. This is not a systematically derived method but is attractive due to its simplicity. It is included here for the purpose of comparison with the 2-parameter method.

A. 1-parameter and Ad hoc methods

The negative log-likelihood for these methods are written as

$$-L(\rho) = \sum_{i=1}^{n_d} h_i(f_S([G_1\rho]_i)),$$

$$h_i(t) \triangleq (b_i e^{-t} + r_i) - y_i \log(b_i e^{-t} + r_i),$$

$$G_1 \triangleq \begin{cases} G & \text{Ad hoc method} \\ G(I_S + AI_B) & \text{1-parameter method.} \end{cases}$$

The function h_i appears in Poisson transmission tomography problems and a quadratic surrogate for it was computed in [4]. The problem is regularized by adding an edge-preserving (Huber) penalty function to the negative log-likelihood to create the final cost function. The cost function can be reduced monotonically by the use of quadratic surrogates [4]. Using the optimal curvatures computed in [4], the surrogate is expressed

as

$$Q_1(\rho; \rho^{(n)}) = \sum_{i=1}^{n_d} h_i(f_S([G_1\rho^{(n)}]_i)) + h'_i(f_S([G_1\rho^{(n)}]_i)) \times (f_S([G_1\rho]_i) - f_S([G_1\rho^{(n)}]_i)) + \frac{1}{2} \tilde{c}_i (f_S([G_1\rho]_i) - f_S([G_1\rho^{(n)}]_i))^2.$$

Observations of $f_S(T_S)$ suggest that it is a concave function. Using Lemmas 3 and 4 of [4] we can prove the following :

$$f'_S(T_S^{(n)})(T_S - T_S^{(n)}) \geq f_S(T_S) - f_S(T_S^{(n)}),$$

$$\left| \frac{f_S(T_S^{(n)})}{T_S^{(n)}} \right| |T_S - T_S^{(n)}| \geq |f_S(T_S) - f_S(T_S^{(n)})|.$$

Observations of $f_S(T_S)$ also suggest that $f'_S(0) \geq \left| \frac{f_S(T_S^{(n)})}{T_S^{(n)}} \right|$. Thus, we have the final form for the surrogate :

$$Q_2(\rho; \rho^{(n)}) = \sum_{i=1}^{n_d} h_i(f_S([G_1\rho^{(n)}]_i)) + h'_i(f_S([G_1\rho^{(n)}]_i)) \times f'_S([G_1\rho^{(n)}]_i) [G_1(\rho - \rho^{(n)})]_i + \frac{1}{2} \tilde{c}_i (f'_S(0))^2 [G_1(\rho - \rho^{(n)})]_i^2.$$

A conjugate gradient method is used to reduce the value of $Q_2(\rho; \rho^{(n)})$ at every iteration. These methods will not have nice convergence properties like monotonicity due to the beam-hardening approximations made to the exact measurement model and the use of masks I_S and I_B . A certain number of iterations are run and the iterate with the best image quality is taken as the final reconstruction. The 1-parameter method is initialized with a 1-parameter JS reconstruction and the Ad hoc method is initialized with a water-corrected FBP reconstruction.

B. 2-parameter and Exact methods

The negative log-likelihood for these methods are written as

$$-L(\rho) = \sum_{i=1}^{n_d} h_i(f([GI_S\rho]_i, [GI_B\rho]_i)).$$

It might be possible to derive an exact 2-D surrogate for this negative log-likelihood along the lines of [4] but the procedure appears to be very complicated. A simpler way is to approximate $f(T_S, T_B)$ by a local Taylor series expansion for every pair of (T_S^n, T_B^n) at the current iterate and hope that this approximation holds for the step sizes generated.

$$f(T_S, T_B) \approx f(T_S^n, T_B^n) + \begin{bmatrix} \dot{f}_{1,0}(T_S^n, T_B^n) & \dot{f}_{0,1}(T_S^n, T_B^n) \end{bmatrix} \begin{bmatrix} T_S - T_S^n \\ T_B - T_B^n \end{bmatrix}.$$

The quadratic approximation can be now written as :

$$Q_3(\rho; \rho^{(n)}) = K + (G_2^T \dot{\mathbf{h}})^T (\rho - \rho^{(n)}) + \frac{1}{2} (\rho - \rho^{(n)})^T G_2^T \text{diag}(\check{c}_i) G_2 (\rho - \rho^{(n)}),$$

$$[\dot{\mathbf{h}}]_i \triangleq \dot{h}_i(f([GI_S \rho^{(n)}]_i, [GI_B \rho^{(n)}]_i)),$$

$$G_2 \triangleq \begin{bmatrix} \text{diag}(\dot{f}_{1,0}) & \text{diag}(\dot{f}_{0,1}) \end{bmatrix} \begin{bmatrix} G & 0 \\ 0 & G \end{bmatrix} \begin{bmatrix} I_S \\ I_B \end{bmatrix}.$$

The problem is regularized by adding an edge-preserving (Huber) penalty function to the negative log-likelihood and a conjugate gradient method is used to reduce the value of the surrogate at every iteration. Due to the Taylor series expansion and use of masks, these algorithms are not guaranteed to be monotonic. However, they have been found to perform satisfactorily in practice. The 2-parameter method is initialized by a 2-parameter JS reconstruction and the Exact method is initialized by a JS method using the water and bone correction table.

1-parameter and Ad hoc methods require one forward projection and one back-projection every iteration. The 2-parameter and Exact methods require two forward and back-projections every iteration.

V. SIMULATION SETUP

A 2-D fan-beam X-ray CT scanner was simulated. The geometry of the scanner is similar to the central slice of a GE Lightspeed Pro scanner. Sinogram data was collected over a 360° rotation over a 50cm field-of-view (FOV). The sinogram dimensions were 984 angles by 888 bins per angle. An 80kVp spectrum was used and the blank scan count summed over the entire X-ray spectrum was 1.1×10^6 per bin. r_i were set to zero for this study. The phantom size was 1024×1024 pixels and the reconstruction was done on a 256×256 grid. A 1024 size grid permits the phantom to have an average bone mineral width of about 1.5mm.

VI. RESULTS AND DISCUSSION

The reconstruction from the water-corrected FBP method (Fig. 4 and Fig. 5) is noisy and contains a streak artifact in the center of the image. The 1-parameter method (Fig. 6) provides a reconstruction which is free from noise but it still contains the streak. The reconstruction from the 2-parameter method (Fig. 7) is rid of the noise as well as the streak artifact. The image quality is comparable to that of the Exact method (Fig. 8). The Ad hoc method (Fig. 9) provides an image quality slightly worse than the 2-parameter method. The 2-parameter method should be the method of choice when compared to the Ad hoc method as it follows the measurement model more closely and uses the same beam-hardening information (water-correction table and tuning parameters).

ACKNOWLEDGMENT

The authors would like to thank GE Healthcare Technologies for providing images and information about a clinical CT scan of a human head and information about the GE Lightspeed Pro scanner.

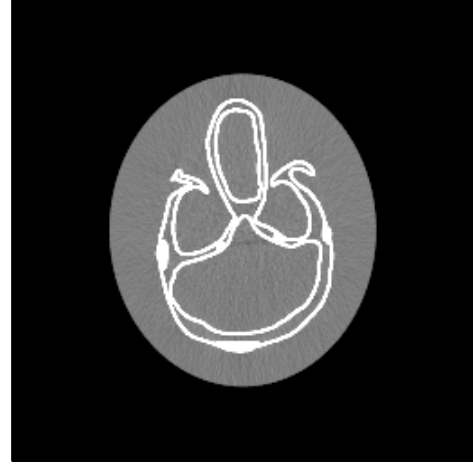


Fig. 4. Water-corrected FBP reconstruction.

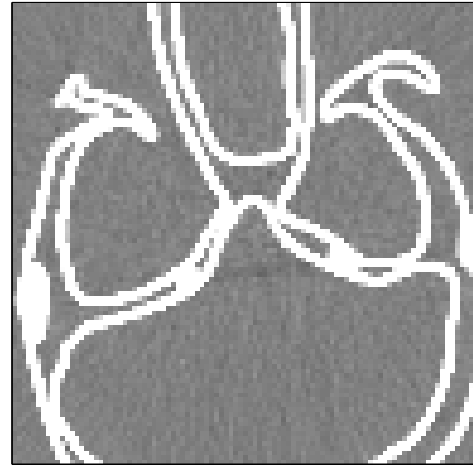


Fig. 5. Water-corrected FBP reconstruction (zoomed in).

REFERENCES

- [1] P. M. Joseph and R. D. Spital, "A method for correcting bone induced artifacts in computed tomography scanners," *J. Comp. Assisted Tomo.*, vol. 2, pp. 100–8, Jan. 1978.
- [2] B. De Man, J. Nuyts, P. Dupont, G. Marchal, and P. Suetens, "An iterative maximum-likelihood polychromatic algorithm for CT," *IEEE Tr. Med. Im.*, vol. 20, no. 10, pp. 999–1008, Oct. 2001.
- [3] I. A. Elbakri and J. A. Fessler, "Statistical image reconstruction for polyenergetic X-ray computed tomography," *IEEE Tr. Med. Im.*, vol. 21, no. 2, pp. 89–99, Feb. 2002.
- [4] H. Erdoğan and J. A. Fessler, "Monotonic algorithms for transmission tomography," *IEEE Tr. Med. Im.*, vol. 18, no. 9, pp. 801–14, Sept. 1999.

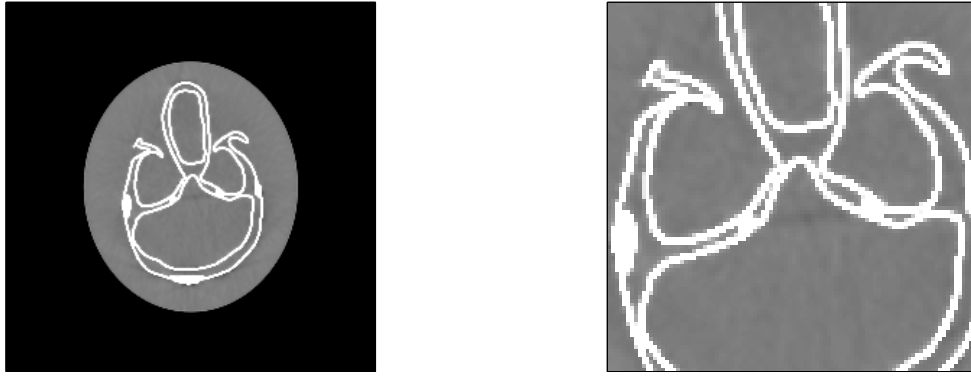


Fig. 6. Reconstruction using the 1-parameter method. Window = 400HU. Left, full image. Right, central part of the image.



Fig. 7. Reconstruction using the 2-parameter method. Window = 400HU. Left, full image. Right, central part of the image.



Fig. 8. Reconstruction using the Exact method. Window = 400HU. Left, full image. Right, central part of the image.



Fig. 9. Reconstruction using the Ad hoc method. Window = 400HU. Left, full image. Right, central part of the image.